Preprints of the 19th World Congress
The International Federation of Automatic Control
Cape Town, South Africa. August 24-29, 2014

Model Predictive Control of Buoy Type Wave Energy Converter

Mohsen N. Soltani * **Mahdi T. Sichani** **
Mahmood Mirzaei ***

* *Aalborg University, Esbjerg, 6700 Denmark (e-mail: sms@et.aau.dk)*
** *Aalborg University, Aalborg, 9220 Denmark (e-mail:mts@civil.aau.dk)*
*** *Technical University of Denmark, Kongens Lyngby, 2800 Denmark (e-mail: mmir@dtu.dk)*

Abstract: The paper introduces the Wavestar wave energy converter and presents the implementation of model predictive controller that maximizes the power generation. The ocean wave power is extracted using a hydraulic electric generator which is connected to an oscillating buoy. The power generator is an additive device attached to the buoy which may include damping, stiffness or similar terms hence will affect the dynamic motion of the buoy. Therefore such a device can be seen as a closed-loop controller. The objective of the wave energy converter is to harvest as much energy from sea as possible. The straight forward solution to this maximization problem is achieved by maximizing the instantaneous range of motion of the buoy. The buoy as a single degree of freedom oscillator will undergo its maximum movements when it is in resonance with the sea state. Hence the best solution to the problem is achieved by forcing this condition. In the paper the theoretical framework for this principal is shown. The optimal controller requires information of the sea state for infinite horizon which is not applicable. Model Predictive Controllers (MPC) can have finite horizon which crosses out this requirement. This approach is then taken into account and an MPC controller is designed for a model wave energy converter and implemented on a numerical example. Further, the power outtake of this controller is compared to the optimal controller as an indicator of the performance of the designed controller.

Keywords: Wave Energy, Buoy, Model Predictive Control, Optimal Control.

1. INTRODUCTION

Various types of Wave Energy Converters (WEC) have been designed in the last decades with the aim of extracting energy of the waves in different sea states [1]. These designs spread over a wide range of concepts. Nevertheless most of them extract energy from the varying sea surface elevation. For example the Pelamis Wave Power Ltd. (2013) uses several submerged tubes interconnected with hinges which have hydraulic power take-off systems inside and convert the relative motion of the joints to the electricity. Oyster WEC has a flap connected to a base at sea bed through two hydraulic pistons which pump water with high pressure to a conventional hydroelectric turbine which finally converts the pressure to electric power, cf. Aquamarine Power (2011). A wavestar device has floaters on the surface of the sea extracting energy using hydraulic pumps connected to an electricity generator Wavestar A/S (2013).

The focus of this paper is on modelling and maximization of the power outtake of a Wavestar point energy converter. The device uses a controller device to convert the motion of its buoy to electrical power. In principal a point absorber can be modelled as a Single Degree Of Freedom (SDOF) oscillating system which oscillates in response to the external loads caused by the change of the sea surface elevation. The power outtake of the device is proportional to its Range Of Motion (ROM) i.e. larger range of motion will result in higher power outtake. Clearly a SDOF oscillator will have its maximum ROM when it is in resonance with its excitation. Therefore the maximum power outtake of the device is obtained when device is in resonance with the sea state.

Sea surface elevation is in principal an irregular process in time and space. Therefore the hydrodynamic load on the device is a stochastic process. This inculcates that stochastic control strategies may be used in order to control the motion of the device and maximize its Power Take Off (PTO). This is elaborated in this paper and results have been presented. Several control strategies for maximization of the electrical power outtake of the point WECs have been proposed in Nielsen et al. (2013); Sichani et al. (2013). Nielsen et al. (2013) have shown that the global optimal power outtake of the device can be obtained once the total information of the incoming waves are available i.e. a controller with infinite horizon. However since this is not a practical assumption a sub-optimal controller is proposed in Sichani et al. (2013) which uses a closed loop control system and utilizes only the available information of the system states at each time.

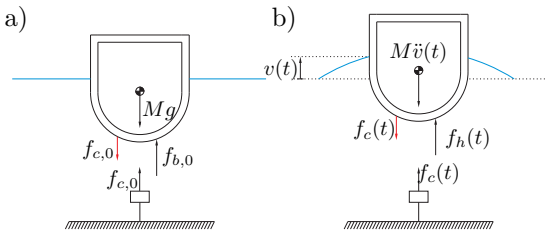

Fig. 1. Schematic view of the buoy. a) Static equilibrium, b) Dynamic equilibrium.

On the other hand a Model Predictive Controller (MPC) has the ability to use the sea state prediction in order to maximize the power during the prediction horizon. Requirements for sea state prediction is widely discussed in Schoen et al. (2011). In Fusco and Ringwood (2012) and Fusco and Ringwood (2010), different prediction algorithms for short term wave forecasting are presented. Linear and non-linear MPC for different types of wave energy absorbers are introduced in Cretel et al. (2011); Brekken (2011); Hals et al. (2010); Richter et al. (2013), where it is indicated that the MPC is a promising controller for increasing the power outtake of WECs.

In this paper, the PTO of MPC is compared to that of the conventional gain controller as well as a global optimal controller. The comparison is also made for MPC with different prediction lengths to justify the benefit of applying MPC. The results show that the PTO for MPC with prediction horizon of 10s and longer will be very close to the PTO of the optimal controller that produces 10% more power than the conventional gain controller.

This paper is organized as follows. In section 2, the model of the Wavestar WEC is presented. The implementation of the model predictive controller is explained in section 3. Section 4 describes the optimal control law, and the section 4 compares the achieved results by means of simulation.

2. MODELING OF WAVE ENERGY CONVERTER

The schematic model of the WEC is shown in figure 1. The equation of motion of the WEC is written around the static equilibrium point where equation (1) applies, c.f. figure 1.a,

$$\begin{aligned} Mg &= f_{b,0} - f_{c,0} \\ f_{b,0} &= \rho V(v(0))g \end{aligned} \tag{1}$$

where $f_{b,0}$ is the buoyancy force where the device is resting at the Mean Water Level (MWL); V is the volume of the displaced water; ρ is the density of the water; g is the acceleration of gravity and $f_{c,0}$ is a possible force from the controller at this position. Invoking the D'Alambert's principal, c.f. figure 1.b, and assuming the viscous force on the buoy is negligible the equation of motion reads

$$\begin{aligned} M\ddot{v}(t) &= f_h(t) - f_c(t) \\ f_h(t) &= f_e(t) + f_r(t) + f_b(t) \end{aligned} \tag{2}$$

where M is the mass of the WEC, $f_c(t)$ is the control force; $f_h(t)$ is the summation of the hydrodynamic forces; $f_e(t)$ is the external excitation force due to the incident waves; $f_r(t)$ is the radiation force of the buoy due to its oscillations in the water and $f_b(t)$ is the buoyancy force of the buoy which is equal to the weight of the displaced water by the device. Note that once the buoy is completely immersed in water the buoyancy force is constant. Lets introduce ϑ as the immersion displacement of the buoy i.e. the value of $v(t)$ for which the buoy is completely immersed in water. As long as $v(t) > \vartheta$ the buoyancy force is written as

$$f_b(t) = -\rho\big(V(v(t)) - V(v(0))\big)g = r(v(t)) \tag{3}$$

where g is the acceleration of gravity. This is a nonlinear buoyancy force, a linear approximation of which can be achieved assuming that the cross section of the buoy does not change with $v(t)$, hence

$$f_b(t) = -\rho A g v(t) = -kv(t) \tag{4}$$

where A is the cross sectional area of the buoy. The total buoyancy force then becomes

$$f_b(t) = \begin{cases} -kv(t) & , \ v(t) > \vartheta \\ -k\vartheta & , \ v(t) \leq \vartheta \end{cases} \tag{5}$$

Next, the radiation force can be written as a convolution of the *radiation Impulse Response Function* (IRF) e.g. $h_{r\dot{v}}(t)$ with the velocity of the device $\dot{v}(t)$

$$f_r(t) = -\int_{-\infty}^{\infty} h_{r\dot{v}}(t-\tau)\dot{v}(\tau)\mathrm{d}\tau \tag{6}$$

Since the radiation IRF is causal i.e. $f_r(t) = 0, t < 0$, pivoting on the reality of the radiation IRF which results in $H_{r\dot{v}}(-\omega) = H^*_{r\dot{v}}(\omega)$ where $H_{r\dot{v}}(\omega)$ is the FRF of the radiation force, the following is satisfied

$$h_{r\dot{v}}(t) = \begin{cases} \dfrac{2}{\pi}\displaystyle\int_0^{\infty} \mathrm{Re}\big(H_{r\dot{v}}(\omega)\big)\cos(\omega t)\mathrm{d}\omega \\ -\dfrac{2}{\pi}\displaystyle\int_0^{\infty} \mathrm{Im}\big(H_{r\dot{v}}(\omega)\big)\sin(\omega t)\mathrm{d}\omega \end{cases} , \quad t \geq 0 \tag{7}$$

In general the Kramers-Kroning relations requires that $\lim_{\omega\to\infty} H_{r\dot{v}}(\omega) = 0$ which is not satisfied by the introduced FRF, Falnes (2002). Therefore, a modified FRF $\tilde{H}_r(\omega)$ is introduced. The real and imaginary parts of the radiation FRF are related to the *Hydrodynamic radiation damping*, $C_r(\omega)$, and *Hydrodynamic added mass*, $M_r(\omega)$, as $H_{r\dot{v}}(\omega) = C_r(\omega) + \mathrm{i}\omega M_r(\omega)$, i.e.,

$$C_r(\omega) = \mathrm{Re}\big(H_{r\dot{v}}(\omega)\big) \quad , \quad M_r(\omega) = \frac{1}{\omega}\mathrm{Im}\big(H_{r\dot{v}}(\omega)\big) \tag{8}$$

Since the hydrodynamic damping converges to zero, the modification is only necessary for the hydrodynamic added mass, see Fig. 2. The modified hydrodynamic added mass is proposed as $\tilde{M}_r(\omega) = M_r(\omega) - M_r(\infty)$ and consequently the modified radiation FRF becomes $\tilde{H}_r(\omega) = C_r(\omega) + \mathrm{i}\omega\tilde{M}_r(\omega)$. Next, defining $V'(\omega)$ as the Fourier transform of the *velocity* of the device, the radiation force is obtained, cf. (6), as

$$\begin{aligned} F_r(\omega) &= -H_{r\dot{v}}(\omega)V'(\omega) \\ &= -\big(\tilde{H}_r(\omega) + \mathrm{i}\omega M_r(\infty)\big)V'(\omega) \end{aligned} \tag{9}$$

which can readily be converted to time domain by taking inverse Fourier transform, Faltinsen (1993), i.e.,

$$f_r(t) = -\int_{-\infty}^{\infty} \tilde{h}_{r\dot{v}}(t-\tau)\dot{v}(\tau)\mathrm{d}\tau - M_r(\infty)\ddot{v}(t) \tag{10}$$

Fig. 2 shows the real and imaginary parts of the radiation FRF, used in the numerical model in this article. This FRF is extracted from the WAMIT software, which is based on Boundary Element Method (BEM) as explained in WAMIT Inc. (2011). Clearly the imaginary part of $H_{r\dot{v}}(\omega)$ is not converging toward zero which is cured by the

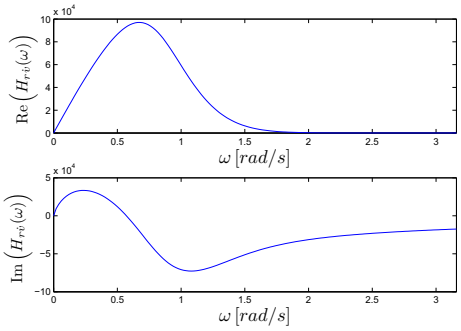

Fig. 2. Real and imaginary parts of the radiation FRF $H_{r\dot{v}}(\omega)$.

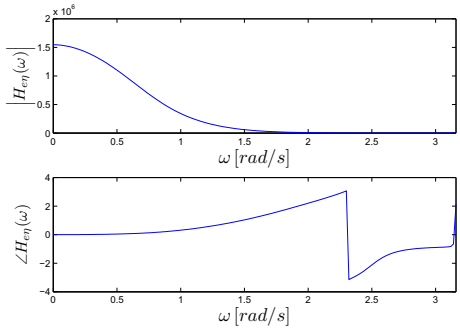

Fig. 3. Magnitude and phase of the excitation FRF $H_{e\eta}(\omega)$.

modification (9). Substituting (4) and (10) in (2) results in the following equation of motion for the WEC

$$m\ \ddot{v}(t) + \int_{-\infty}^{\infty} \tilde{h}_{r\dot{v}}(t-\tau)\dot{v}(\tau)\mathrm{d}\tau + kv(t) = -f_c(t) + f_e(t)$$
$$m = M + M_r(\infty) \tag{11}$$

which can be easily solved using any numerical time integration scheme. The external wave force on the buoy can be calculated as the convolution of its IRF, $h_{e\eta}(t)$, with the wave elevation $\eta(t)$. It is well-known that $h_{e\eta}(t)$ is non-causal hence the information of the wave in front of the buoy is needed to calculate the wave force Falnes (2002). The FRF of the external excitation, $H_{e\eta}(\omega)$, for the buoy under study in this paper is shown in Fig. 3. In order to finalize the modeling part of the paper a stochastic model for the wave elevation, $\eta(t)$, should be available. Here the one-sided JONSWAP spectrum by Hasselmann et al. (1973) and Det Norske Veritas (2010) is used

$$S_\eta(\omega) = A_\gamma S_{PM}(\omega)\gamma^{\exp\left(-0.5\left(\frac{\omega-\omega_p}{\sigma\omega_p}\right)^2\right)} \tag{12}$$
$$S_{PM}(\omega) = \frac{5}{16}H_s^2\omega_p^4\omega^{-5}\exp\left(-\frac{5}{4}\left(\frac{\omega}{\omega_p}\right)^{-4}\right) \tag{13}$$
$$A_\gamma = 1 - 0.287\ln(\gamma) \tag{14}$$
$$\gamma = 3.3 \tag{15}$$
$$\sigma = \begin{cases} 0.07\ , \ \omega \le \omega_p \\ 0.09\ , \ \omega > \omega_p \end{cases} \tag{16}$$

The parameters of the wave spectrum are chosen as the peak frequency of the wave $\omega_p = 0.8434\,[s]$ and the significant wave height of $H_s = 3\,[m]$. The model parameters are chosen $\rho = 1025\,[kg/m^3]$ and $A = 154\,[m^2]$.

3. MODEL PREDICTIVE CONTROL

The transfer function of the radiation damping is obtained by fitting a rational function to the frequency response function of radiation damping. The state-space realization of this transfer function will be of the form

$$\begin{aligned} \dot{\boldsymbol{\xi}}(t) &= \boldsymbol{A}_r\boldsymbol{\xi}(t) + \boldsymbol{B}_r\dot{v}(t) \\ \tilde{f}_r(t) &= \boldsymbol{C}_r\boldsymbol{\xi}(t) + \boldsymbol{D}_r\dot{v}(t), \end{aligned} \tag{17}$$

where $\boldsymbol{\xi}(t) \in \mathbb{R}^l$ is the radiation damping state vector, $\tilde{f}_r(t)$ is the convolution term in (11), and $\boldsymbol{A}_r$, $\boldsymbol{B}_r$, $\boldsymbol{C}_r$, and $\boldsymbol{D}_r$ are the state-space matrices. Substituting (17) in (11), the state-space model of the WEC becomes:

$$\begin{aligned} \frac{d}{dt}\begin{bmatrix} v(t) \\ \dot{v}(t) \\ \boldsymbol{\xi}(t) \end{bmatrix} &= \begin{bmatrix} 0 & 1 & \boldsymbol{0} \\ -\frac{k}{m} & -\frac{1}{m}\boldsymbol{D}_r & -\frac{1}{m}\boldsymbol{C}_r \\ \boldsymbol{0} & \boldsymbol{B}_r & \boldsymbol{A}_r \end{bmatrix}\begin{bmatrix} v(t) \\ \dot{v}(t) \\ \boldsymbol{\xi}(t) \end{bmatrix} + \\ &\begin{bmatrix} 0 \\ -\frac{1}{m} \\ 0 \end{bmatrix} f_c(t) + \begin{bmatrix} 0 \\ \frac{1}{m} \\ 0 \end{bmatrix} f_e(t) \\ y(t) &= \begin{bmatrix} 1 & 0 & 0 \\ 0 & 1 & 0 \end{bmatrix}\begin{bmatrix} v(t) \\ \dot{v}(t) \\ \boldsymbol{\xi}(t) \end{bmatrix}, \end{aligned} \tag{18}$$

The state-space can be discretized using zero-order-hold rule resulting in

$$\begin{aligned} \boldsymbol{z}(k+1) &= \boldsymbol{A}\boldsymbol{z}(k) + \boldsymbol{B}u(k) + \boldsymbol{E}d(k) \\ \boldsymbol{y}(k) &= \boldsymbol{C}\boldsymbol{z}(k), \end{aligned} \tag{19}$$

where $\boldsymbol{z}(k) = [v(k)\ \dot{v}(k)\ \boldsymbol{\xi}(k)^T]^T$, $\boldsymbol{z}(k) \in \mathbb{R}^{l+2}$, $u(k) = f_c(k)$ is the control force, and $d(k) = f_e(k)$ is the wave excitation force. The excitation force can be written as sum of the prediction $\hat{d}(k)$ and the prediction error $\tilde{d}(k)$, $d(k) = \hat{d}(k) + \tilde{d}(k)$. The prediction of the excitation force is obtained from the convolution of $h_{e\eta}(t)$ by the short-term wave elevation forecasting $\hat{\eta}(t)$, as explained in Fusco and Ringwood (2012). The prediction error $\tilde{d}(k)$ is assumed to be a zero mean Gaussian white noise.

The states of the radiation damping are not measurable. However, the radiation damping can be realized as an observable state-space in (17) which makes it possible to design an observer for those states. Thus, an observer for the system (19) will be of the form

$$\hat{\boldsymbol{z}}(k+1) = (\boldsymbol{A} - \boldsymbol{L}\boldsymbol{C})\hat{\boldsymbol{z}}(k) + \boldsymbol{B}u(k) + \boldsymbol{E}\hat{d}(k) + \boldsymbol{L}\boldsymbol{y}(k), \tag{20}$$

where $\boldsymbol{L}$ can be designed as a Kalman gain to minimize the second norm of the estimation error, see Grewal and Andrews (2001). The predictions of the states can be achieved by iterating the model description (19) given by

$$\begin{aligned} \hat{\boldsymbol{z}}(k+i|k) &= \boldsymbol{A}^i\hat{\boldsymbol{z}}(k) + \sum_{j=0}^{i-1}\boldsymbol{A}^j\boldsymbol{B}u(k+j) \\ &+ \sum_{j=0}^{i-1}\boldsymbol{A}^j\boldsymbol{E}\hat{d}(k+j) \text{ for } i = 1,\ 2, ...,\ H_p, \end{aligned} \tag{21}$$

in which H_p is the prediction horizon. Thus, the stacked predicted states will be

$$\hat{\boldsymbol{z}} = \boldsymbol{F}\hat{\boldsymbol{z}}(k) + \boldsymbol{P}\boldsymbol{u} + \boldsymbol{D}\hat{\boldsymbol{d}}, \tag{22}$$

with

$$\hat{\boldsymbol{z}} = (\hat{\boldsymbol{z}}(k+1|k)^T\ \hat{\boldsymbol{z}}(k+2|k)^T\ ...\ \hat{\boldsymbol{z}}(k+H_p|k)^T)^T \tag{23}$$

$$\boldsymbol{u} = (u(k)\ u(k+1)\ ...\ u(k+H_p-1))^T \tag{24}$$

$$\hat{\boldsymbol{d}} = (\hat{d}(k)\ \hat{d}(k+1)\ ...\ \hat{d}(k+H_p-1))^T \tag{25}$$

and the matrices $\boldsymbol{F}$, $\boldsymbol{P}$, and $\boldsymbol{D}$ are defined as

$$\boldsymbol{F} = \begin{bmatrix} \boldsymbol{A}^T & \boldsymbol{A}^{2^T} & \cdots & \boldsymbol{A}^{H_p^T} \end{bmatrix}^T$$

$$\boldsymbol{P} = \begin{bmatrix} \boldsymbol{B} & \boldsymbol{0} & \cdots & \boldsymbol{0} \\ \boldsymbol{AB} & \boldsymbol{B} & \cdots & \boldsymbol{0} \\ \vdots & \vdots & \ddots & \vdots \\ \boldsymbol{A}^{H_p-1}\boldsymbol{B} & \boldsymbol{A}^{H_p-2}\boldsymbol{B} & \cdots & \boldsymbol{B} \end{bmatrix} \tag{26}$$

$$\boldsymbol{D} = \begin{bmatrix} \boldsymbol{E} & \boldsymbol{0} & \cdots & \boldsymbol{0} \\ \boldsymbol{AE} & \boldsymbol{E} & \cdots & \boldsymbol{0} \\ \vdots & \vdots & \ddots & \vdots \\ \boldsymbol{A}^{H_p-1}\boldsymbol{E} & \boldsymbol{A}^{H_p-2}\boldsymbol{E} & \cdots & \boldsymbol{E} \end{bmatrix}.$$

Once the state predictions are computed as a function of control inputs, we can use these predictions in the formulation of the optimization problem.

3.1 Control Objective

The control objective for the WEC system is to maximize the average power outtake during a a time interval T that is of interest. Thus, the objective function will be in the form of

$$\bar{P}_a = \frac{1}{T}\int_0^T P_a(t)dt, \tag{27}$$

where $P_a(t)$ is the instantaneous produced mechanical power given by

$$P_a = f_c(t)\dot{v}(t). \tag{28}$$

The MPC objective function can be formulated as the discrete form of the integral (27) as

$$\bar{P}_a \approx \frac{T_s}{T}\sum_{i=k}^{k+T/T_s} \boldsymbol{z}(i)\boldsymbol{S}u(i), \tag{29}$$

where $\boldsymbol{S} = [0\ \ 1\ \ \boldsymbol{0}]^T$ and T_s is the sampling time. It is also assumed that T is chosen such that T/Ts is an integer. As the future values of $\boldsymbol{z}(k)$ and $u(k)$ are not known, the MPC can be formulated such that the prediction of those variables are used in the objective function, i.e.,

$$J = \hat{\boldsymbol{z}}^T\bar{\boldsymbol{S}}\boldsymbol{u}, \tag{30}$$

in which

$$\bar{\boldsymbol{S}} = \begin{bmatrix} \boldsymbol{S} & \boldsymbol{0} & \cdots & \boldsymbol{0} \\ \boldsymbol{0} & \boldsymbol{S} & \cdots & \boldsymbol{0} \\ \vdots & \vdots & \ddots & \vdots \\ \boldsymbol{0} & \boldsymbol{0} & \cdots & \boldsymbol{S} \end{bmatrix}$$

is a $(l+2)H_p \times H_p$ matrix. The maximization problem of the objective function (30) is a Linear Program (LP) with the state prediction (23) as its equality constraint. However, the equality constraint can be substituted in the objective function (30), resulting in a Quadratic Program (QP) of the form

$$J = \boldsymbol{u}^T\bar{\boldsymbol{Q}}\boldsymbol{u} + \boldsymbol{q}^T\boldsymbol{u}, \tag{31}$$

where $\bar{\boldsymbol{Q}} = \boldsymbol{P}^T\bar{\boldsymbol{S}}$ and $\boldsymbol{q}^T = \hat{\boldsymbol{z}}(k)^T\boldsymbol{F}^T\bar{\boldsymbol{S}} + \hat{\boldsymbol{d}}^T\boldsymbol{D}^T\bar{\boldsymbol{S}}$. The vector $\boldsymbol{q}$ is known at each sampling time, since $\hat{\boldsymbol{z}}(k)$ is provided by the state estimator and $\hat{d}$ is provided from the forecast of the excitation force. The matrix $\bar{\boldsymbol{Q}} + \bar{\boldsymbol{Q}}^T$ is negative definite ($\bar{\boldsymbol{Q}} + \bar{\boldsymbol{Q}}^T \prec 0$), which means that the QP optimization problem has a maximum. The physical interpretation of this concave optimization problem is that the control force and the velocity should act in opposite directions in order to have power outtake. Increasing or decreasing the control force to infinity will end up moving the buoy in the direction of the control force, and thus, resulting in power consumption.

In practice, control force $f_c(t)$ is limited within a threshold ($f_{c,min} \le f_c(t) \le f_{c,max}$), which must be implemented as the inequality constraint of the optimization problem. Thus, the optimization problem to be solved at each sample time will be

$$\begin{aligned} &\text{maximize } \boldsymbol{u}^T\bar{\boldsymbol{Q}}\boldsymbol{u} + \boldsymbol{q}^T\boldsymbol{u} \\ &\text{subject to } \boldsymbol{F}_{c,min} \le \boldsymbol{u} \le \boldsymbol{F}_{c,max}, \end{aligned} \tag{32}$$

where $\boldsymbol{F}_{c,min} = [f_{c,min}\ f_{c,min}\ \cdots\ f_{c,min}]^T$, $\boldsymbol{F}_{c,min} \in \mathbb{R}^{H_p}$ and $\boldsymbol{F}_{c,max} = [f_{c,max}\ f_{c,max}\ \cdots\ f_{c,max}]^T$, $\boldsymbol{F}_{c,max} \in \mathbb{R}^{H_p}$.

4. OPTIMAL CONTROL

The optimal control with a finite horizon for the WEC system can be achieved by solving the following optimization problem

$$\begin{aligned} &\text{maximize } \frac{1}{T}\int_0^T f_c(t)\boldsymbol{S}\boldsymbol{x}(t)dt \\ &\text{subject to } \dot{\boldsymbol{x}}(t) = \boldsymbol{f}(\boldsymbol{x}(t), f_c(t), t) \\ &\qquad\qquad \boldsymbol{x}(0) = \boldsymbol{x}_0, \end{aligned} \tag{33}$$

where $\boldsymbol{x}(t) \in \mathbb{R}^{l+2}$ is

$$\boldsymbol{x}(t) = \begin{bmatrix} v(t) \\ \dot{v}(t) \\ \boldsymbol{\xi}(t) \end{bmatrix}, \tag{34}$$

and the vector function $\boldsymbol{f}$ is

$$\boldsymbol{f}(\boldsymbol{x}(t), f_c(t), t) = \begin{bmatrix} \dot{v}(t) \\ \frac{1}{m}(-r(v(t)) - \boldsymbol{D}_r\dot{v}(t) - \boldsymbol{C}_r\boldsymbol{\xi}(t) + f_e(t) - f_c(t)) \\ \boldsymbol{A}_r\boldsymbol{\xi}(t) + \boldsymbol{B}_r\dot{v}(t) \end{bmatrix}. \tag{35}$$

The optimization problem (33) can be solved by following the Maximum Principle Pontryagin et al. (1964); Boyd and Vanderberghe (2004). The Hamiltonian function is then defined as

$$H(\boldsymbol{x}(t), f_c(t), \boldsymbol{\lambda}(t), t) = f_c(t)\boldsymbol{S}\boldsymbol{x}(t) + \boldsymbol{\lambda}(t)^T\boldsymbol{f}(\boldsymbol{x}(t), f_c(t), t), \tag{36}$$

where $\boldsymbol{\lambda}(t) = (\lambda_1(t)\ \lambda_2(t)\ \boldsymbol{\lambda}_3(t)^T)^T \in \mathbb{R}^{l+2}$ is the co-state vector. Assuming that Hamiltonian is differentiable with respect to the control, the first order conditions to the Hamiltonian are obtained by differentiating Hamiltonian with respect to control, state, and co-state variables as follows

$$\frac{\partial H}{\partial f_c} = 0 \qquad \textit{Stationarity condition}, \tag{37}$$

$$\dot{\boldsymbol{x}}(t) = \frac{\partial H}{\partial \boldsymbol{\lambda}} \qquad \textit{Equation of motion for } \boldsymbol{x}(t), \tag{38}$$

$$\dot{\boldsymbol{\lambda}}(t) = -\frac{\partial H}{\partial \boldsymbol{x}} \qquad \textit{Equation of motion for } \boldsymbol{\lambda}(t), \tag{39}$$

$$\boldsymbol{\lambda}(T) = \boldsymbol{0} \qquad \textit{Transversality condition}. \tag{40}$$

Using (35) and (36) in the stationarity condition (37) will result in

$$\lambda_2(t) = m\dot{v}(t). \tag{41}$$

The equation of motion for $\boldsymbol{\lambda}(t)$ will be obtained from (39) as

$$\dot{\lambda}_1(t) = -\frac{\partial H}{\partial v} = -\frac{d}{dv} r(v(t)) \frac{\lambda_2(t)}{m} \tag{42}$$

$$\dot{\lambda}_2(t) = -\frac{\partial H}{\partial \dot{v}} = -(f_c(t) + \lambda_1(t) - \boldsymbol{D}_r \frac{\lambda_2(t)}{m} - \boldsymbol{B}_r^T \boldsymbol{\lambda}_3(t)) \tag{43}$$

$$\dot{\boldsymbol{\lambda}}_3(t) = -\frac{\partial H}{\partial \boldsymbol{\xi}} = -\boldsymbol{A}_r^T \boldsymbol{\lambda}_3(t) + \boldsymbol{C}_r^T \frac{\lambda_2(t)}{m}. \tag{44}$$

Substituting (41) in (42), we will get

$$\dot{\lambda}_1(t) = -\frac{d}{dv} r(v(t)) \dot{v}(t) = -\frac{d}{dt} r(v(t)). \tag{45}$$

The solution of this differential equation has to satisfy the transversality condition (40) resulting in

$$\lambda_1(t) = r(v(t)) - r(v(T)). \tag{46}$$

By substituting (41) and its derivative as well as (46) into (43), the control force can be obtained as

$$\begin{cases} f_c(t) &= -m\ddot{v}(t) - r(v(t)) + r(v(T)) + \boldsymbol{D}_r \dot{v}(t) + \boldsymbol{B}_r^T \boldsymbol{\lambda}_3(t) \\ \dot{\boldsymbol{\lambda}}_3(t) &= -\boldsymbol{A}_r^T \boldsymbol{\lambda}_3(t) + \boldsymbol{C}_r^T \dot{v}(t). \end{cases} \tag{47}$$

The terminal condition $v(T) = 0$ is chosen to erase the static control force $r(v(T))$, and thus, keep the static equilibrium point as explained in (1). Furthermore, the transversality condition (40) should be satisfied for $\boldsymbol{\lambda}_3(T)$. Thus the optimal control force can be written in convolution form as

$$f_c(t) = -m\ddot{v}(t) - r(v(t)) + \int_t^T (\boldsymbol{C}_r e^{-\boldsymbol{A}_r(t-\tau)} \boldsymbol{B}_r + \boldsymbol{D}_r) \dot{v}(\tau) d\tau. \tag{48}$$

By substituting (48) into the equation of motion (11), we can obtain the convolution term as

$$\int_t^T (\boldsymbol{C}_r \; e^{-\boldsymbol{A}_r(t-\tau)} \boldsymbol{B}_r + \boldsymbol{D}_r) \dot{v}(\tau) d\tau = f_e(t) - \int_0^t (\boldsymbol{C}_r e^{-\boldsymbol{A}_r(t-\tau)} \boldsymbol{B}_r + \boldsymbol{D}_r) \dot{v}(\tau) d\tau. \tag{49}$$

This will form the optimal control law as

$$\begin{cases} f_c(t) = -m\ddot{v}(t) - r(v(t)) + r(v(T)) + f_e(t) \\ \qquad -\boldsymbol{D}_r \dot{v}(t) - \boldsymbol{B}_r^T \boldsymbol{\lambda}_3(t) \\ \dot{\boldsymbol{\lambda}}_3(t) = -\boldsymbol{A}_r^T \boldsymbol{\lambda}_3(t) + \boldsymbol{C}_r^T \dot{v}(t) \\ \dot{v}(0) = \dot{v}_0 \end{cases} \tag{50}$$

5. RESULTS

Three controllers are implemented on the buoy wave energy absorber model (2)-(11) of the Wavestar WEC: The model predictive controller as explained in section 3, the optimal control law as explained in section 4, and a velocity feedback controller $f_c(t) = C_c \dot{v}(t)$, where the optimal gain C_c is obtained in Nielsen et al. (2013). The comparison is done for one generated time series of wave elevation. The instantaneous generated power is compared in Fig. 4 for three controllers. The comparison shows that optimal control law, which maximizes the power, produces more negative values compared to MPC. The negative values can be interpreted as the power that is consumed by the absorber to produce a specific force. In other words, the negative power is the one that is fed to the buoy from the hydraulic generator making the buoy both producer and user of the energy. The

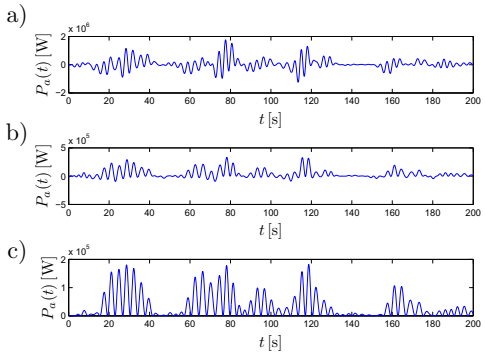

Fig. 4. Instantaneous power of the WEC with different controllers; a) Optimal controller, b) MPC, c) Optimal gain controller

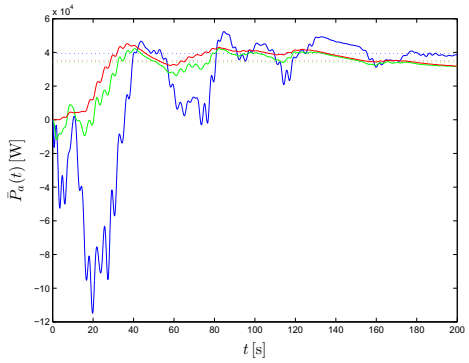

Fig. 5. Convergence of the harvested power of the WEC with different controllers; blue: Optimal controller , green: MPC with $H_p = 50$, red: Optimal gain controller, dashed lines: mean power

feedback controller does not consume energy from the generator since it has only a dissipative term $C_c \dot{v}(t)$ that absorbs the power from the wave, i.e., $P(t) = f_c(t)\dot{v}(t) = C_c \dot{v}(t)^2$. Another interesting result, is that MPC has the lower peak instantaneous power compared to the optimal controller. This is an important factor when sizing the generator for a wave absorber. The mean and cumulative produced power for three controllers are shown in Fig. 5. The MPC with prediction horizon of 50 samples (with sampling time of 0.1s) is used in this comparison. The mean generated power by the optimal controller is shown to be the highest, whereas the mean generated power for feedback controller is slightly higher than the MPC with prediction horizon of 50. In Fig. 6, the performance of the optimal controller is compared to MPC with three different lengths of prediction horizon: 10, 50, and 100 samples. It is observed that the mean produced power in MPC will be very close to that of the optimal controller when MPC has a long prediction horizon. Eventually, an statistical analysis of the MPC performance for different lengths of prediction horizon is done. Fifty random realizations of the sea state of length 200s are generated. All 50 sea states are tested for 41 predictive controllers with different prediction horizons and the statistical results of 2050 tests are revealed in Fig. 7. Each point in this figure is the average of the mean power production in 50 random sea states. The results show that long prediction horizons will

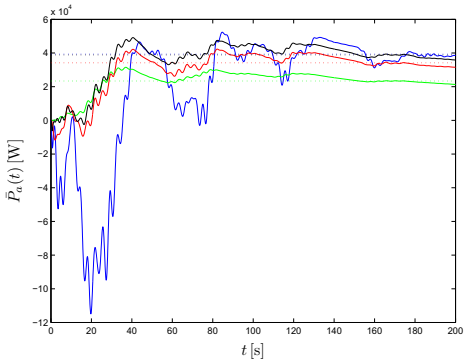

Fig. 6. Convergence of the harvested power of the WEC with different controllers; blue: Optimal controller , green: MPC with $H_p = 10$, red: MPC with $H_p = 50$, black: MPC with $H_p = 100$ dashed lines: mean power

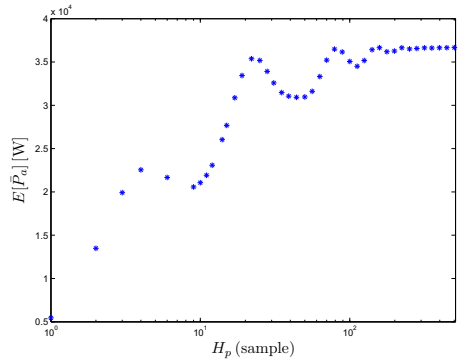

Fig. 7. Average of the mean power in 50 different sea states for MPC with different prediction horizons.

result in high profit. However, $H_p \geq 100$ samples will not result in a significant benefit in terms of produced power.

6. CONCLUSION

In this paper, a model predictive controller is compared to the optimal controller for wave energy converter in order to justify what prediction horizons are suitable for a finite horizon MPC. The results of the implemented MPC on a Wavestar absorber showed that the power outtake for prediction horizon of 10 seconds is very close to that of the optimal controller and longer prediction horizons does not make a significant change in the power outtake. The optimal controller showed to be able to produce 10% more power than the conventional gain controller. Since the optimal controller with infinite horizon is not practically feasible, the finite horizon MPC seems to be a qualified candidate for this type of WEC.

7. ACKNOWLEDGEMENT

The second author gratefully acknowledge the support from the Nordic Council of Ministers for the grant 11-01949-16 within sustainable and renewable energy.

REFERENCES

Aquamarine Power (2011). How oyster wave power works. URL `www.aquamarinepower.com`.

Boyd, S.P. and Vanderberghe, L. (2004). *Convex Optimization*. Cambridge University Press.

Brekken, T.K.A. (2011). On model predictive control for a point absorber wave energy converter. In *PowerTech, 2011 IEEE Trondheim*, 1–8.

Cretel, J.A.M., Lightbody, G., Thomas, G.P., and Lewis, A.W. (2011). Maximisation of energy capture by a wave-energy point absorber using model predictive control. In *IFAC World Congress*, 3714–3721.

Det Norske Veritas (2010). Recommended practice: "environmental conditions and environmental loads". Technical Report DNV-RP-C205, Det Norske Veritas.

Falnes, J. (2002). *Ocean Waves and Oscillating Systems: Linear Interactions Including Wave-Energy Extraction*. Cambridge University Press, 1st edition.

Faltinsen, O. (1993). *Sea loads on ships and offshore structures*. Cambridge University Press.

Fusco, F. and Ringwood, J.V. (2010). Short-term wave forecasting with ar models in real-time optimal control of wave energy converters. In *Industrial Electronics (ISIE), 2010 IEEE International Symposium on*, 2475–2480.

Fusco, F. and Ringwood, J.V. (2012). A study of the prediction requirements in real-time control of wave energy converters. *Sustainable Energy, IEEE Transactions on*, 3(1), 176–184.

Grewal, M.S. and Andrews, A.P. (2001). *Kalman Filtering*. Prentice Hall, Inc., second edition.

Hals, J., Falnes, J., and Moan, T. (2010). Constrained optimal control of a heaving buoy wave-energy converter. *Journal of Offshore Mechanics and Arctic Engineering*, 133(1), 011401.

Hasselmann, K., Barnett, T.P., Bouws, E., Carlson, H., Cartwright, D.E., Enke, K., Ewing, J.A., Gienapp, H., Hasselmann, D.E., Kruseman, P., Meerburg, A., M"uller, P., Olbers, D.J., Richter, K., Sell, W., and Walden, H. (1973). Measurements of wind-wave growth and swell decay during the joint north sea wave project (jonswap). report, Deutches Hydrographisches Institut.

Nielsen, S.R.K., Zhou, Q., Kramer, M.M., Basu, B., and Zhang, Z. (2013). Optimal control of nonlinear wave energy point converters. *Ocean Engineering*, 72(0), 176 – 187.

Pelamis Wave Power Ltd. (2013). Pelamis wave. URL `www.pelamiswave.com`.

Pontryagin, L.S., Boltyanskii, V.G., Gamkrelitze, R.V., and Mishenko, E.F. (1964). *The Mathematical Theory of Optimal Processes*. MacMillan, New York.

Richter, M., Magana, M.E., Sawodny, O., and Brekken, T.K.A. (2013). Nonlinear model predictive control of a point absorber wave energy converter. *Sustainable Energy, IEEE Transactions on*, 4(1), 118–126.

Schoen, M.P., Hals, J., and Moan, T. (2011). Wave prediction and robust control of heaving wave energy devices for irregular waves. *Energy Conversion, IEEE Transactions on*, 26(2), 627–638.

Sichani, M.T., Chen, J.B., Li, J., Kramer, M.M., and Nielsen, S.R.K. (2013). Constrained optimal stochastic control of non-linear wave energy point absorbers. *submitted to Applied Ocean Research*, (0).

WAMIT Inc. (2011). WAMIT user manual, version 7.0. report. URL `www.wamit.com`.

Wavestar A/S (2013). URL `www.wavestarenergy.com`.